Radiotherapy and Oncology 159 (2021) 265–276

Contents lists available at ScienceDirect

Radiotherapy and Oncology

journal homepage: www.thegreenjournal.com

Original Article

Impact of DNA repair and reactive oxygen species levels on radioresistance in pancreatic cancer

Lily Nguyen [a,b], Sophie Dobiasch [a,b,c], Günter Schneider [d,e], Roland M. Schmid [d], Omid Azimzadeh [f], Kristiyan Kanev [g], Dominik Buschmann [g], Michael W. Pfaffl [g], Stefan Bartzsch [a,b], Thomas E. Schmid [a,b], Daniela Schilling [a,b], Stephanie E. Combs [a,b,c,*]

[a] Institute of Radiation Medicine (IRM), Department of Radiation Sciences (DRS), Helmholtz Zentrum München, Neuherberg; [b] Department of Radiation Oncology, School of Medicine, Klinikum rechts der Isar, Technical University of Munich (TUM); [c] Deutsches Konsortium für Translationale Krebsforschung (DKTK), Partner Site Munich, Munich; [d] Department of Medicine II, School of Medicine, Klinikum rechts der Isar, Technical University of Munich (TUM); [e] Deutsches Krebsforschungszentrum (DKFZ) and German Cancer Consortium (DKTK), Heidelberg; [f] Institute of Radiation Biology (ISB), Department of Radiation Sciences (DRS), Helmholtz Zentrum München, Neuherberg; and [g] Division of Animal Physiology and Immunology, TUM School of Life Sciences Weihenstephan, Technical University of Munich (TUM), Freising, Germany

ARTICLE INFO

Article history:
Received 30 September 2020
Received in revised form 29 March 2021
Accepted 29 March 2021
Available online 09 April 2021

Keywords:
Pancreatic cancer
Radioresistance
RNA sequencing
Migration
Invasion

ABSTRACT

Purpose: Radioresistance in pancreatic cancer patients remains a critical obstacle to overcome. Understanding the molecular mechanisms underlying radioresistance may achieve better response to radiotherapy and thereby improving the poor treatment outcome. The aim of the present study was to elucidate the mechanisms leading to radioresistance by detailed characterization of isogenic radioresistant and radiosensitive cell lines.

Methods: The human pancreatic cancer cell lines, Panc-1 and MIA PaCa-2 were repeatedly exposed to radiation to generate radioresistant (RR) isogenic cell lines. The surviving cells were expanded, and their radiosensitivity was measured using colony formation assay. Tumor growth delay after irradiation was determined in a mouse pancreatic cancer xenograft model. Gene and protein expression were analyzed using RNA sequencing and Western blot, respectively. Cell cycle distribution and apoptosis (Caspase 3/7) were measured by FACS analysis. Reactive oxygen species generation and DNA damage were analyzed by detection of CM-H_2DCFDA and γH2AX staining, respectively. Transwell chamber assays were used to investigate cell migration and invasion.

Results: The acquired radioresistance of RR cell lines was demonstrated *in vitro* and validated *in vivo*. Ingenuity pathway analysis of RNA sequencing data predicted activation of cell viability in both RR cell lines. RR cancer cell lines demonstrated greater DNA repair efficiency and lower basal and radiation-induced reactive oxygen species levels. Migration and invasion were differentially affected in RR cell lines.

Conclusions: Our data indicate that repeated exposure to irradiation increases the expression of genes involved in cell viability and thereby leads to radioresistance. Mechanistically, increased DNA repair capacity and reduced oxidative stress might contribute to the radioresistant phenotype.

Pancreatic cancer is a devastating disease with a 5-year survival rate of less than 5% [1]. It is the 8th leading cause of cancer-related deaths; moreover, it is expected to be the second most common cause by 2030 [2,3]. So far, the only curative treatment option for pancreatic cancer is the complete surgical resection of the tumor; yet, at the time of diagnosis, only 10–20% of patients present a locally resectable disease and are eligible for surgery [4]. Around 50% of the patients present with advanced disease, including distant metastases, and in about one-third of all patients, a locally advanced, but non-metastasized disease is diagnosed [5,6]. For the latter patients, neoadjuvant therapy combining chemotherapy and radiotherapy offers an opportunity to downstage borderline resectable and locally advanced tumors and thus, improve not only resection rates but also overall survival [6,7]. The major aim of local radiotherapy is to achieve loco-regional disease control, and tumor downsizing, as well as the prevention of tumor cell dissemination and invasion.

Nonetheless, the combined therapy often fails due to the inherent chemo- and radioresistant nature of pancreatic cancer, limiting the efficacy and outcome [8]. To date, no randomized trial has

* Corresponding author at: Department of Radiation Oncology, School of Medicine, Klinikum rechts der Isar, Technical University of Munich (TUM), Ismaninger Str. 22, 81675 Munich, Germany.
E-mail address: stephanie.combs@tum.de (S.E. Combs).

https://doi.org/10.1016/j.radonc.2021.03.038
0167-8140/

shown the superiority of radiotherapy alone or in combination with chemotherapy to chemotherapy alone [6,7] in primarily unresectable pancreatic cancer, while newer studies argue for the benefit of intensified chemotherapy with FOLFIRINOX (oxaliplatin, irinotecan, fluorouracil, and leucovorin), especially in borderline-resectable tumors [9,10]. A close look at the data of most clinical studies reveals that only ~30% of pancreatic cancer patients show a response to radiation therapy [11–14].

It appears that the main reason for all trials showing no advantage of the treatment with radiotherapy in primarily unresectable pancreatic cancer may be due to the missing information about the individual radiation sensitivity [15,16].

Radioresistance is a process in which tumor cells develop mechanisms to withstand radiation–induced cell death. Ionizing radiation leads to DNA double-strand breaks (DSB) by either damaging it directly or through the production of free radicals, e.g., reactive oxygen species (ROS) [17,18]. Upon DNA damage, cells initiate the DNA damage response (DDR) involving DNA damage sensing and transduction pathways, cell cycle arrest and DNA repair. Activation of cell cycle checkpoints by DNA damage leads to cell cycle arrest and thereby allowing time for DNA repair [19]. Tumor cells - which are mostly p53 mutated and hence defective in the G1 checkpoint - mainly rely on the G2/M checkpoint after radiation-induced DNA damage, leading to accumulation in the G2-phase [20].

The vast majority of radiation-induced DNA DSBs is caused by ROS. Scavenging systems, including superoxide dismutases (SOD), glutathione peroxidase, peroxiredoxin, glutaredoxin, thioredoxin, and catalase prevent the accumulation of ROS [21]. Therefore, increased levels of these antioxidants diminish radiation-induced ROS levels and subsequently lead to decreased DNA damage and thereby contribute to radioresistance.

Altogether, the balance between ROS-induced DNA damage and DDR can determine the success of radiation treatment [22]. Targeting DDR signaling pathways to improve cancer therapy is currently investigated in many clinical studies in combination with radiotherapy [23]. Furthermore, ROS elevating anticancer drugs have shown promising results *in vitro* and *in vivo* [24].

However, the detailed mechanisms that contribute to radioresistance in pancreatic cancer remain mostly unknown. Moreover, clinical data suggest a heterogeneous and patient-specific response to radiation treatment, which may be due to individual radiosensitivity or radioresistance. Therefore, the aim of the present study was to establish an *in vitro* isogenic model of radioresistant pancreatic cancer cells and to comprehensively characterize the cellular phenotype to elucidate the mechanisms leading to radioresistance.

Materials and Methods

Cells and cell culture

The human pancreatic cancer cell lines Panc-1 and MIA PaCa-2 were obtained from Deutsche Sammlung von Mikroorganismen und Zellkulturen (DSMZ) and cultured in DMEM supplemented with 10% FCS and 1% P/S. All cells were kept at 37 °C in a controlled atmosphere with 5% CO2 and 95% humidity. Cells were routinely checked and determined as negative for mycoplasma contamination (MycoAlert, Lonza).

Establishment of radioresistant (RR) cell lines and irradiation

The RR cell lines Panc-1 RR and MIA PaCa-2 RR were generated from the human parental cell lines Panc-1 and MIA PaCa-2 (both p53 mutants) [25], as previously described with minor modifications [26]. Cells were irradiated with 2 Gy using the RS225A irradiation device (Gulmay/Xstrahl, Camberley, UK) at a dose rate of 1 Gy/min (15 mA, 200 kV). Cells were then subcultured into new flasks. When cells reached 70% confluency, cells where serially irradiated with increasing doses (4, 6, and 8 Gy) and additional six cycles of 10 Gy radiation (Fig. 1A). In order to obtain age-matched parental cell lines, Panc-1 and MIA PaCa-2 cells were subcultured for the same period but without irradiation. These "high-passage" cell lines were used as controls in all experiments. The authenticity of the RR and age-matched parental cell lines was confirmed by cell line authentication test (Eurofins).

Colony formation assay

Cells were seeded in 12-well plates, and 24 h later irradiated with a single dose of radiation ranging from 0 to 8 Gy. After 11–15 days, colonies were fixed with ice-cold methanol, stained with 0.1% crystal violet and counted. Colonies consisting of more than 50 single cells were counted as one colony with the GelCountTM (Oxford Optronics, Abingdon, UK). Survival curves were fitted according to the linear-quadratic model (LQM) with the equation $SF = -\alpha \times D - \beta \times D^2$ using GraphPad Prism (GraphPad Software Inc., San Diego, USA). All survival curves were constructed from at least three independent experiments.

In vivo studies

All animal experiments were approved by the government of Upper Bavaria, Germany, and conducted according to the German animal protection guidelines. For tumor xenografts, 4×10^6 cells suspended in PBS were injected subcutaneously into the right flank of 7–8 week old, female athymic CD1-Foxn1 nude mice (Charles River Laboratories, Germany). Treatment of tumor-bearing mice was initiated when tumors reached a size of 60–100 mm^3, at which point mice were randomized into the untreated or radiotherapy treatment group. Mice were irradiated with 5 or 10 Gy using Small Animal Radiation Research Platform (SARRP, XStrahl), a high-precision small animal irradiator equipped with a cone-beam CT (CBCT) scanner. The tumor size was measured with a digital caliper 3 times a week and its volume (mm^3) was approximated by $V = length \times (width)^2 \times \frac{\pi}{6}$. The tumor growth over time t after treatment was fitted to an exponential function, $V(t) = V_0 e^{\alpha t}$, with parameters V_0 and α. The time when the tumor reached four times its volume at treatment is denoted as $t = T_4$ and was calculated using $T_4 = \ln(4)/\alpha$. The tumor growth delay is defined as the T_4 difference between control and irradiated animals. Animals were sacrificed once the tumor reached a size of 1 cm in one dimension.

RNA sequencing

RNA was extracted from cultured cells using the miRNeasy Mini Kit (Qiagen). RNA libraries were generated with the NEBNext Ultra RNA Library Prep Kit for Illumina (New England Biolabs Inc.), according to the manufacturer's protocol. The samples were sequenced on an Illumina HiSeq 2500 system with the following conditions: rapid run, 100-bp single-end reads, dual-indexed sequencing.

Sequencing data for mRNA were processed using the snakemake pipeline (v0.5) (https://gitlab.lrz.de/ImmunoPhysio/bulkSeq-Pipe). The quality of sequencing data was assessed using fastqc (v.1.2) prior to clipping adaptor sequences using trimmomatic (v.0.36). STAR (v.2.7.1a) was used to align reads to the genome build 38 with annotation 95. Mapped reads were counted using htseq (v.0.9.1). Differential expression analysis was performed using R (v.3.6.1) and the Bioconductor package DESeq2 (v.1.24.0) with the included median ratios of mean expression-based normalization and false discovery correction according to Benjamini-Hochberg. Read counts were modelled as a negative binomial dis-

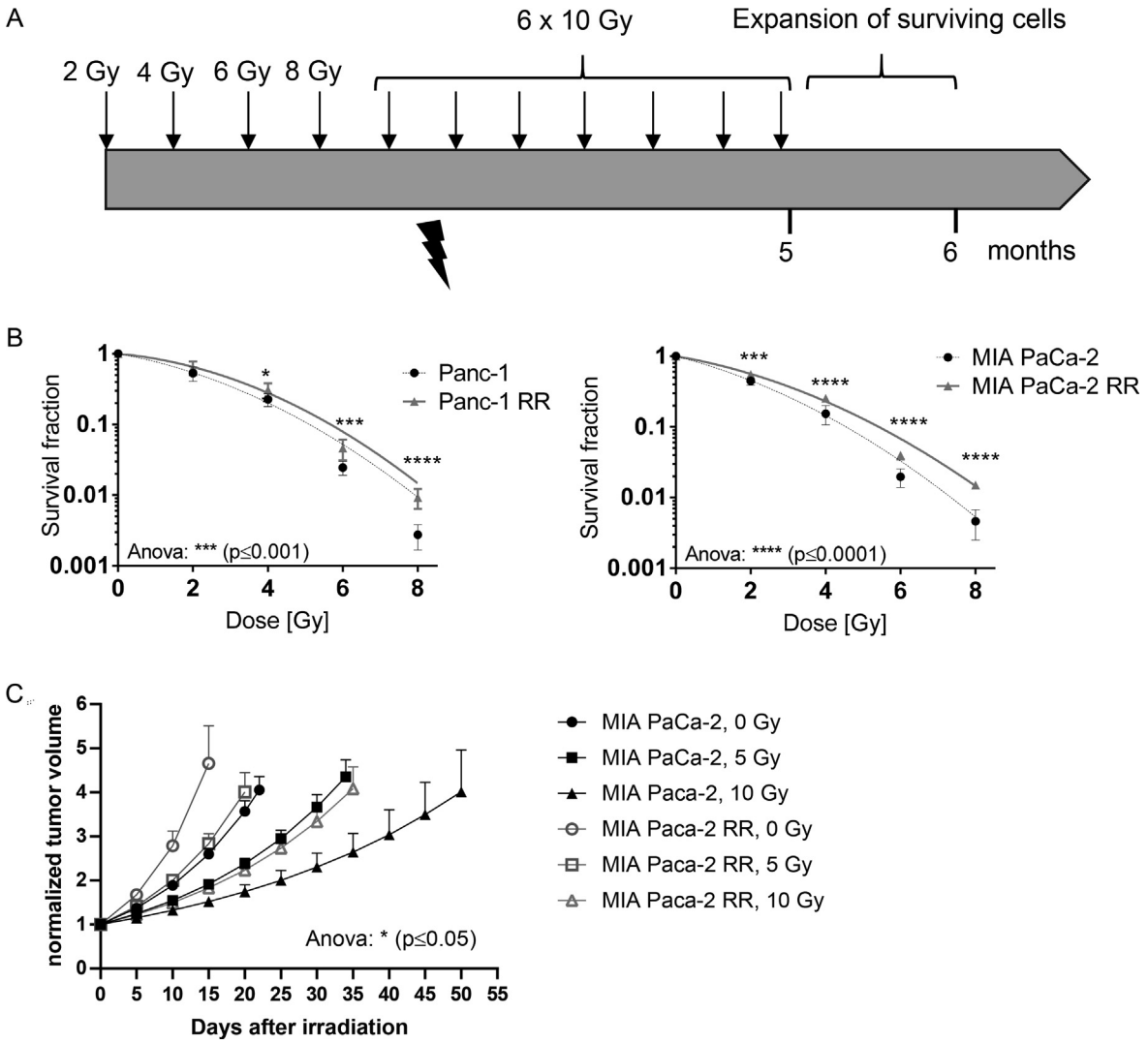

Fig. 1. Generation of radioresistant sublines surviving multiple fractions of radiation. **A.** Scheme for the establishment of radioresistant (RR) pancreatic cancer cell lines. Cells were serially irradiated with increasing doses (2, 4, 6, and 8 Gy) and additional six cycles of 10 Gy radiation. **B.** Clonogenic survival of Panc-1 and MIA PaCa-2 and their respective RR cell lines. One day after seeding, cells were irradiated with 2, 4, 6, and 8 Gy. Sham irradiated cells served as control (0 Gy). Data are expressed as mean ± SD of at least 3 independent experiments (two-way ANOVA; ***$p \leq 0.001$, ****$p \leq 0.0001$; Student's t-test; *$p \leq 0.05$, ***$p \leq 0.001$, ****$p \leq 0.0001$). **C.** Relative tumor growth of MIA PaCa–2 RR and MIA PaCa–2 parental cells. Cells were injected subcutaneously into nude mice and then treated with irradiation as indicated. The normalized tumor volumes were plotted against the number of days ($n \geq 6$ per group; two-way ANOVA; *$p \leq 0.05$).

tribution with estimated mean values and gene-specific dispersion parameters. Thresholds of Log2 fold change $\geq |1|$, adjusted p-value ≤ 0.05 and baseMean ≥ 50 were set to identify significantly regulated transcripts. Pathway analysis on deregulated mRNAs were performed by the software tool INGENUITY Pathway Analysis (IPA) (QIAGEN Inc., https://www.qiagenbioinformatics.com/products/ingenuity-pathway-analysis).

Cell cycle analysis

Cell cycle distributions were analyzed using propidium iodide (PI) and flow cytometry. Exponentially growing cells were grown in complete medium and harvested 24 h after irradiation with 8 Gy. Sham irradiated cells served as control (0 Gy). Cells were fixed with ice-cold 70% ethanol for at least 2 h at −20 °C. Afterwards, cells were stained with PI in the presence of RNase and analyzed on a FACSCalibur flow cytometer. The cell cycle distribution was calculated using Modfit software (Verity Software House Inc, Topsham, USA).

γH2AX staining (Flow Cytometry)

Detection of γH2AX by FACS was performed according to Tanaka et al. [27]. Cells were fixed 30 min after irradiation with 1% PFA at 4 °C and resuspended in 70% ethanol. Cells were then incubated with a mouse anti-human anti–phospho–histone H2AX (ser139) antibody (Millipore) for 2 h at room temperature. Cells were incubated with Alexa Fluor 488-labeled goat anti-mouse secondary antibody (Invitrogen) for 30 min at room temperature in the dark. After washing, cells were incubated with PI and RNase A for 30 min at room temperature and analyzed on a FACSCalibur (BD Biosciences, San Jose, USA) flow cytometer. Relative mean fluorescence intensity (MFI) values were calculated since the basal fluorescence intensities varied in different antibody lots.

γH2AX staining (Immunofluorescence)

Cells were fixed 24 h after irradiation with 2% PFA for 15 min. Cells were then washed, permeabilized with Triton X-100, and incubated with anti-human anti-phospho-histone H2AX (ser139)

antibody (Millipore) overnight at 4 °C. Cells were washed and incubated with Alexa Fluor 488 labeled goat anti-mouse secondary antibody (Invitrogen) for 1 hour at room temperature in the dark. Foci from at least 100 cells were counted manually for each sample.

Measurement of intracellular ROS

Intracellular ROS levels were measured by CM-H_2DCFDA (Thermo Fisher, Waltham, USA) and flow cytometry. Cells were incubated in PBS containing 10 μM CM-H_2DCFDA for 30 min at 37 °C. After irradiation, cells were immediately placed on ice and analyzed with a flow cytometer.

Cell migration and invasion assay

Cell migration and invasion assays were performed using transwell chambers (8 μm pore sized control inserts and matrigel coated inserts, respectively). Cells in medium supplemented with 0.5% serum and medium containing 10% serum were added to the upper and lower compartment of the insert, respectively. After 24 h at 37 °C, cells on the lower side of the insert were fixed with ice-cold methanol and stained with 0.1% crystal violet. Cells from six randomly selected microscopic views were automatically counted using ImageJ.

Western blot analysis

The cells were lysed using RIPA buffer and the protein concentration was measured by the Bradford assay. Immunoblot analysis was performed using anti-p21 (#2947, Cell Signaling), anti-CDC2 (#9116, Cell Signaling), anti-Cyclin B1 (#4135, Cell Signaling), anti-CDC25C (#4688, Cell Signaling), anti-WEE1 (#4936, Cell Signaling), anti-ß-actin (A5316, Sigma), anti-phospho-NRF2 (phospho S40) (#ab76026, Abcam), anti-NRF2 (#ab62352, Abcam), anti-SOD2/MnSOD (#ab13533, abcam), anti-SOD1 (#ab13498, abcam), anti-TRX (#ab133524, abcam), and anti-GAPDH (#5174, cell signaling).

Statistics

Statistical analysis was performed using GraphPad Prism software (Version 8.0.2, San Diego, USA). Statistical significance of clonogenic survival between parental and radioresistant cell lines was determined using two-way ANOVA and Student's t-test. The tumor growth delay results were evaluated using a two-way ANOVA. Student's t-test was used to determine significant differences between parental and radioresistant cell lines for all other assays. A p-value of ≤ 0.05 was considered to be statistically significant ($^{*}p \leq 0.05$, $^{**}p \leq 0.01$, $^{***}p \leq 0.001$, $^{****}p \leq 0.0001$).

Results

We established two radioresistant (RR) pancreatic cancer cell lines, Panc-1 RR and MIA PaCa–2 RR, through repeated exposure to ionizing radiation (IR) with a cumulative dose of 80 Gy (Fig. 1A). To assess the radiosensitivity of the established RR cell lines compared with parental cells, colony formation assays were performed. As shown in Fig. 1B, RR cells demonstrated significantly higher levels of clonal survival after irradiation (two-way ANOVA $p < 0.001$ and t-test as indicated in the figure). Survival curve data were further analyzed using the linear-quadratic model, and the radiobiological parameters are presented in detail in Table S1. D_{10}, D_{37} and D_{50} values were significantly higher in Panc-1 RR and MIA PaCa-2 RR than in their respective parental cells confirming the enhanced radioresistance. Importantly, cellular growth rates and calculated doubling times indicated that the RR cells and the parental cell lines possess similar proliferation rates *in vitro* (Table S2).

A tumor growth delay experiment was carried out using MIA PaCa–2 and MIA PaCa–2 RR tumors growing subcutaneously in the hind leg of nude mice. Fig. 1C depicts the growth of control (0 Gy) and irradiated tumors following a single dose of 5 or 10 Gy. Non-irradiated MIA PaCa–2 RR tumors showed a significant decrease in time to reach 4-fold volume compared to non-irradiated MIA PaCa–2 tumors (Fig. S1) indicating that tumors from RR cells exhibit faster growth *in vivo*. Irradiated tumors arising from MIA PaCa–2 RR cells exhibited a significantly shorter growth delay than their parental counterparts (Fig. 1C and Table S3). These results suggest that the generated RR cells also exhibit higher radioresistance *in vivo*.

To investigate the underlying molecular basis of the radioresistant phenotype, mRNA sequencing was conducted. Principal component analysis of mRNA expression distinguished RR cells from parental cell lines (Fig. 2A). 609 significantly deregulated mRNAs and 1102 significantly deregulated mRNAs were identified in MIA PaCa-2 RR and Panc-1 RR cells, respectively. Among deregulated mRNAs, 121 mRNAs were commonly affected between Panc-1 RR and MIA PaCa–2 RR cells when compared with their parental cell lines (Fig. 2B). Further analysis of these shared differentially regulated mRNAs using Ingenuity Pathway Analysis (IPA) revealed a predicted activation of cell viability in both RR cell lines (Fig. 2C). The 18 differentially regulated mRNAs that predicted the activation of cell viability are depicted in Fig. 2C and listed in Table S4. Some of these genes (e.g., *CDKN1A, HIPK2, SHH, AHR, ABCC3)* are known for their role in apoptosis, cell cycle distribution, DNA damage repair, and ROS generation [28–32]. As all these molecular networks contribute to radiation response and cell survival, the radioresistant cell lines were characterized in terms of radiation–induced apoptosis, cell cycle distribution, DNA damage repair, and ROS generation.

Induction of apoptosis by a radiation dose of 8 Gy was determined by the detection of caspase 3/7 activity. A significant induction of apoptosis was observed in MIA PaCa-2 and MIA PaCa–2 RR cells 48 h post-irradiation (Fig. S2). However, no significant differences between parental and RR cells were observed. These results suggest that alterations in apoptosis induction are unlikely to account for the radioresistant phenotype in Panc-1 RR and MIA PaCa–2 RR cells.

RNA sequencing analysis demonstrated that cyclin-dependent kinase inhibitor 1 (*CDKN1A or p21*) is upregulated in Panc-1 RR and MIA PaCa–2 RR cells (Fig. 2C and Table S4). CDKN1A inhibits cyclin-dependent kinase 1 (CDK1 or CDC2) and thereby plays a role in cell cycle regulation [33]. Therefore, cell cycle distribution of parental and RR cells without radiation and in response to radiation was analyzed by PI staining and flow cytometry.

Interestingly, the basal non-irradiated fractions of the RR Panc-1 and MIA PaCa-2 cells are significantly elevated in the G2/M phase when compared with the parental cells (Fig. 3A and Fig. S3). To elucidate the mechanisms contributing to the increased G2/M phase in RR cells, the expression of proteins, involved in cell cycle control was analysed by Western Blot (Fig. 3B and 3C). In line with the RNA sequencing data, the expression of p21 is significantly increased in RR Panc-1 and MIA PaCa-2 cells compared to the parental cells. Whereas the expression of WEE1 kinase does not differ between parental and RR MIA PaCa-2 cell lines, WEE1 expression is diminished in RR Panc-1 cells. The expression of the phosphatase CDC25C, the cyclin dependent kinase CDK1 (CDC2) and Cyclin B1 is significantly reduced in both RR cell lines. The deregulated expression of p21 (up), CDC25C (down), CDC2 (down) and Cyclin B1 (down) might cause the G2/M increase in RR cells.

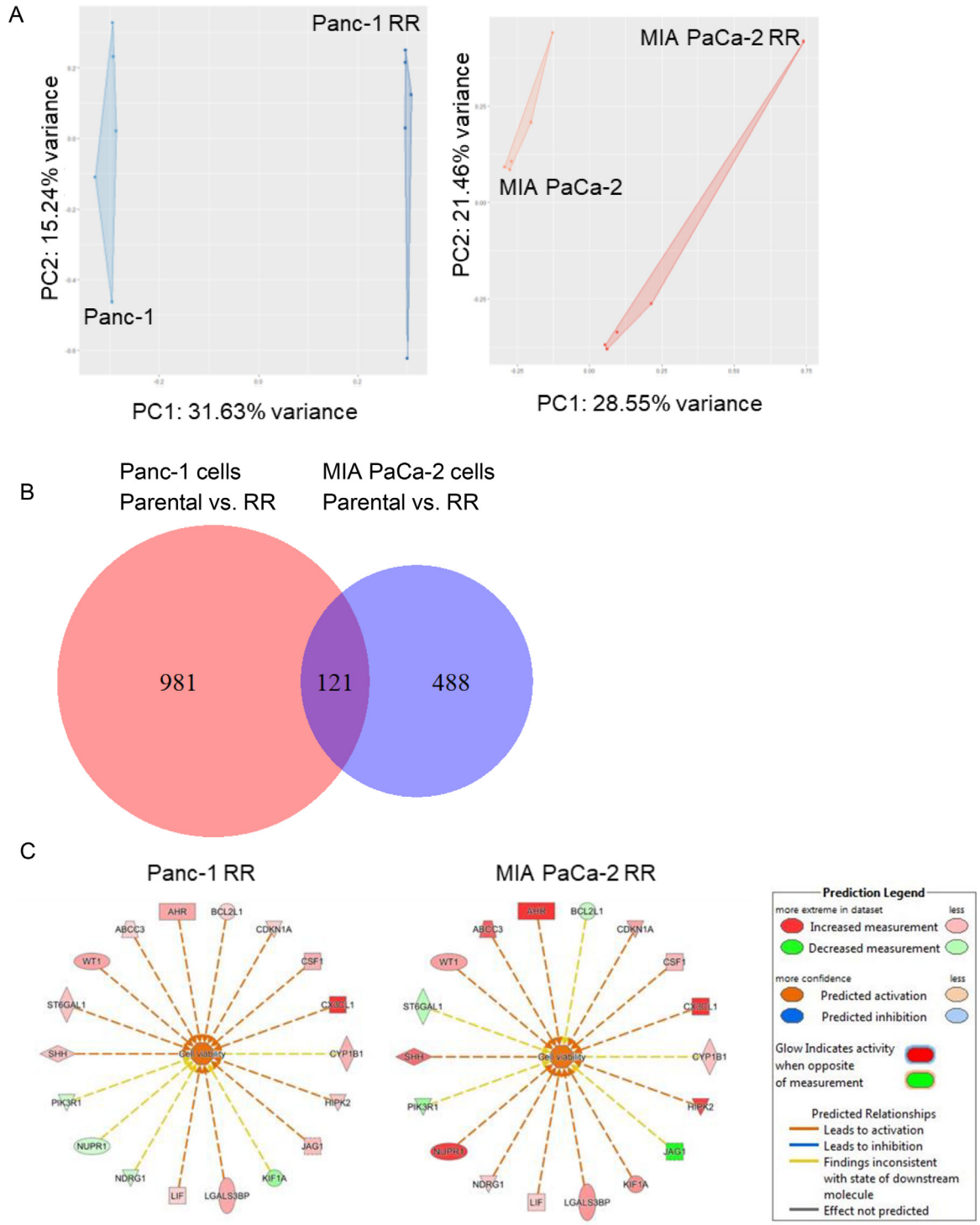

Fig. 2. Transcriptome analysis of parental and RR cell lines. A. Principal component analysis of mRNA expression in Panc-1 and MIA PaCa-2 as well as their RR cells. **B.** Comparative gene expression profiling of Panc-1 and MIA PaCa–2 cells and their respective RR cell lines. Venn diagrams show an overlap in the sets of genes significantly deregulated between Panc–1 and Panc–1 RR cells in comparison with MIA PaCa–2 and MIA PaCa–2 RR cells. **C.** IPA prediction of the activation of cell viability based on the shared deregulated genes from RNA sequencing between parental and RR cell lines. The upregulated genes are marked in red and the down-regulated genes in green. The orange color of the node (cell viability) indicates activation. The gene IDs and log2 fold change are available in Table S4.

As expected, irradiation with 8 Gy induced a G2/M arrest in all cell lines (Fig. S3). The radiation-induced G2/M arrest was significantly more pronounced in the parental cell lines (Panc-1: 3.20-fold, MIA PaCa-2: 3.24-fold) than in the RR cell lines (Panc-1 RR: 1.43-fold, MIA PaCa-2 RR: 2.47-fold) (Fig. 3D). This might be caused by an increased radiation-induced DNA damage in parental cells.

Therefore, radiation-induced DNA damage and the DNA double-strand break (DSB) repair were investigated by detection of γH2AX by flow cytometry (Fig. 4A and Fig. S4) and immunofluorescence (Fig. 4B) 30 min and 24 h after irradiation, respectively. The basal level of phosphorylated γH2AX was similar in both MIA PaCa-2 and MIA PaCa-2 RR cells, Panc-1 RR cells showed lower levels than their parental cell line. Radiation-induced γH2AX formation

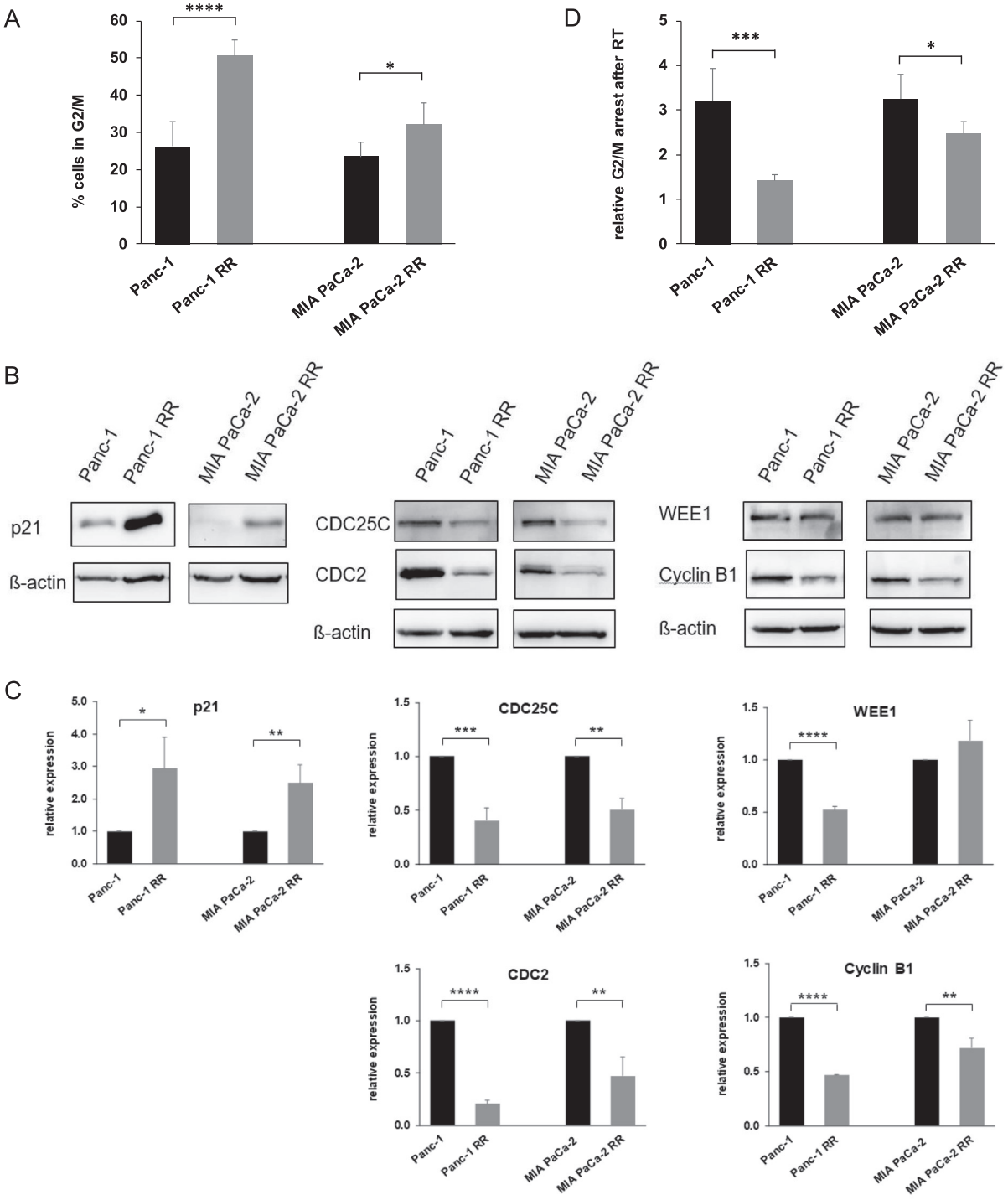

Fig. 3. Cell cycle distribution in parental and RR cell lines. A. Cell cycle distribution was determined in unirradiated cells. Cells were stained with PI and cell cycle distribution was measured by flow cytometry. Quantification of cells in G2/M phase is shown for Panc-1 and Panc–1 RR, MIA PaCa-2 and MIA PaCa-2 RR. Data are expressed as mean ± SD of at least 3 independent experiments (Student's t-test; $^{*}p \leq 0.05$, $^{****}p \leq 0.0001$). **B.** Representative western blot showing the expression of p21, CDC25C, CDC2, WEE1, Cyclin B1 and ß-actin in parental and RR Panc-1 and MIA PaCa-2 cells. **C.** Quantification of Western blot analysis. Image Lab (Bio-Rad) was used to quantify the bands in relation to the loading control ß-actin. The graph represents the quantification of proteins relative to ß-actin and normalized to the respective parental cell line. Data are expressed as mean ± SD of 3 independent experiments (Student's t-test; $^{*}p \leq 0.05$, $^{**}p \leq 0.01$, $^{***}p \leq 0.001$, $^{****}p \leq 0.0001$). **D.** Cell cycle distribution was determined 24 h after irradiation with 8 Gy. Cells were stained with PI and cell cycle distribution was measured by flow cytometry. Relative induction of cells in G2/M phase 24 h after irradiation with 8 Gy in relation to unirradiated cells is shown for Panc-1 and Panc–1 RR, MIA PaCa-2 and MIA PaCa-2 RR. Data are expressed as mean ± SD of at least 3 independent experiments (Student's t-test; $^{*}p \leq 0.05$, $^{**}p \leq 00.1$).

30 min post-irradiation was seen in all cell lines; however, the level of γH2AX in Panc–1 RR was significantly lower when compared to parental Panc-1 cells (Fig. 4A). To investigate whether the increased radioresistance is due to higher DNA DSB repair, we used fluorescence staining of γH2AX 24 h post-irradiation. Without irradiation, parental and RR cells displayed similar levels of γH2AX foci. 24 h after irradiation with a dose of 8 Gy, both Panc-1 RR and MIA PaCa-2 RR cells had significantly lower levels

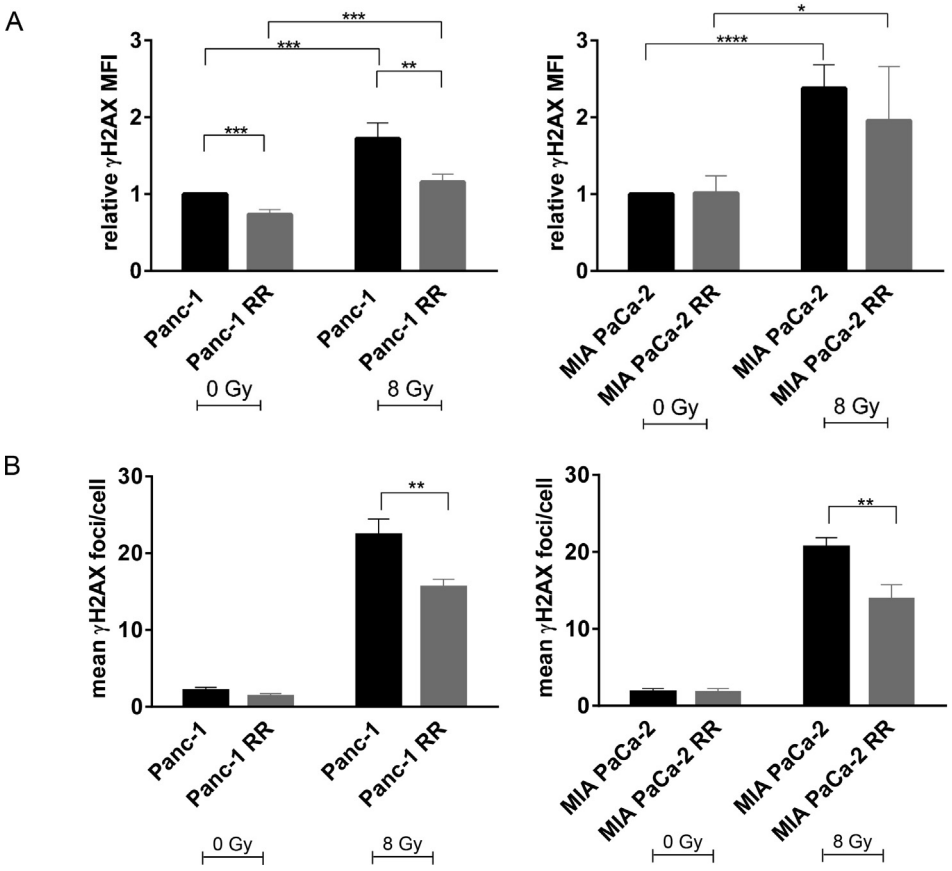

Fig. 4. X-Ray-induced DNA damage is reduced in radioresistant (RR) cell lines. A. Parental and RR MIA PaCa-2 and Panc-1 cells were irradiated with 8 Gy. Unirradiated cells (0 Gy) served as a control. 30 min post-irradiation cells were fixed, stained for γH2AX, and the mean fluorescence intensity (MFI) was measured by flow cytometry. MFI values for each cell line were normalized to the MFI obtained for the respective unirradiated parental cell line. Data are expressed as mean ± SD of at least 3 independent experiments (Student's t-test; $^{*}p \leq 0.05$, $^{**}p \leq 0.01$, $^{***}p \leq 0.001$, $^{****}p \leq 0.0001$). **B.** Quantitative analysis of the number of γH2AX foci per cell. Parental and RR MIA PaCa-2 and Panc-1 cells were irradiated with 8 Gy. Unirradiated cells (0 Gy) served as a control. 24 h post-irradiation cells were fixed and stained for γH2AX. Foci were analyzed by fluorescence microscopy. Data are expressed as mean ± SD of at least 3 independent experiments (Student's t-test; $^{**}p \leq 0.01$).

of γH2AX foci as compared to parental cells (Fig. 4B). Altogether, the present findings reveal lower radiation-induced DNA damage and a greater capacity to repair DNA DSB in RR cells.

Reactive oxygen species (ROS) are one of the mediators that contribute to DNA damage and DNA damage response. Therefore, we determined whether alterations in ROS levels contribute to the radioresistance of Panc-1 RR and MIA PaCa-2 RR cells. Intracellular ROS levels were measured with CM-H_2DCFDA and flow cytometry. The basal levels of ROS were significantly reduced in untreated Panc–1 RR and MIA PaCa-2 RR cells when compared to their respective parental cell line (Fig. 5A) indicating less oxidative stress. Radiation significantly induced ROS in all four cell lines. However, the level of radiation-induced ROS was significantly lower in Panc-1 RR and MIA PaCa-2 RR cells when compared to their respective parental cell line. These results suggest that low basal and reduced radiation-induced ROS levels are involved in the radioresistance of Panc-1 RR and MIA PaCa-2 RR cells.

Western blot analysis was performed to analyse the expression of proteins involved in the oxidative stress pathway. Whereas nuclear factor erythroid 2-related factor 2 (NRF2) was not differentially expressed, superoxide dismutase 1 (SOD1), superoxide dismutase 2 (SOD2), thioredoxin (TRX), and phosphorylated NRF2 (p-NRF2) were significantly up-regulated in Panc-1 RR cells compared to parental cells (Fig. 5B and 5C). In MIA PaCa-2 parental and RR cell lines, no significant differences in the protein expression levels were observed. These data let assume that the enhanced expression of SOD1, SOD2, TRX and p-NRF2 might contribute to the reduced ROS levels in RR Panc-1 cells.

IPA analysis of commonly shared deregulated genes between the two RR cell lines also predicted changes in their migratory and invasive capacities (Fig. 6A, Table S5). Whereas IPA predicted activation of migration and invasion in the Panc–1 RR cells when compared to their parental cell line, migration and invasion were predicted to be decreased in MIA PaCa–2 RR cells. These changes are supposed to be mainly mediated by the increase or decrease of annexin A1 (*ANXA1*), BCL2 like 1 (*BCL2L1*), and N-myc downstream regulated 1 (*NDRG1*). For the validation of the prediction from IPA, transwell migration and invasion assays with parental and RR cell lines were performed. Panc–1 RR cells showed an increase in migration and invasion, while MIA PaCa–2 RR cells showed a reduction when compared to their parental cell lines (Fig. 6B-C). To confirm these data, a wound healing assay was performed showing significantly enhanced migration after 24 h in Panc-1 RR cells compared to parental cells (Fig. S5). These functional data confirm the IPA prediction and indicate that the radiation-induced changes in RR cells differentially affect their invasion and migration capacity.

Discussion

For patients with locally advanced but non-metastasized tumors local radiotherapy, in combination with chemotherapy, can lead to effective downstaging, and in about 30% of these patients, secondary resectability can be achieved [34–36] and thereby the overall survival rate is improved [37,38]. However, only one-third of locally advanced tumors respond to radiotherapy

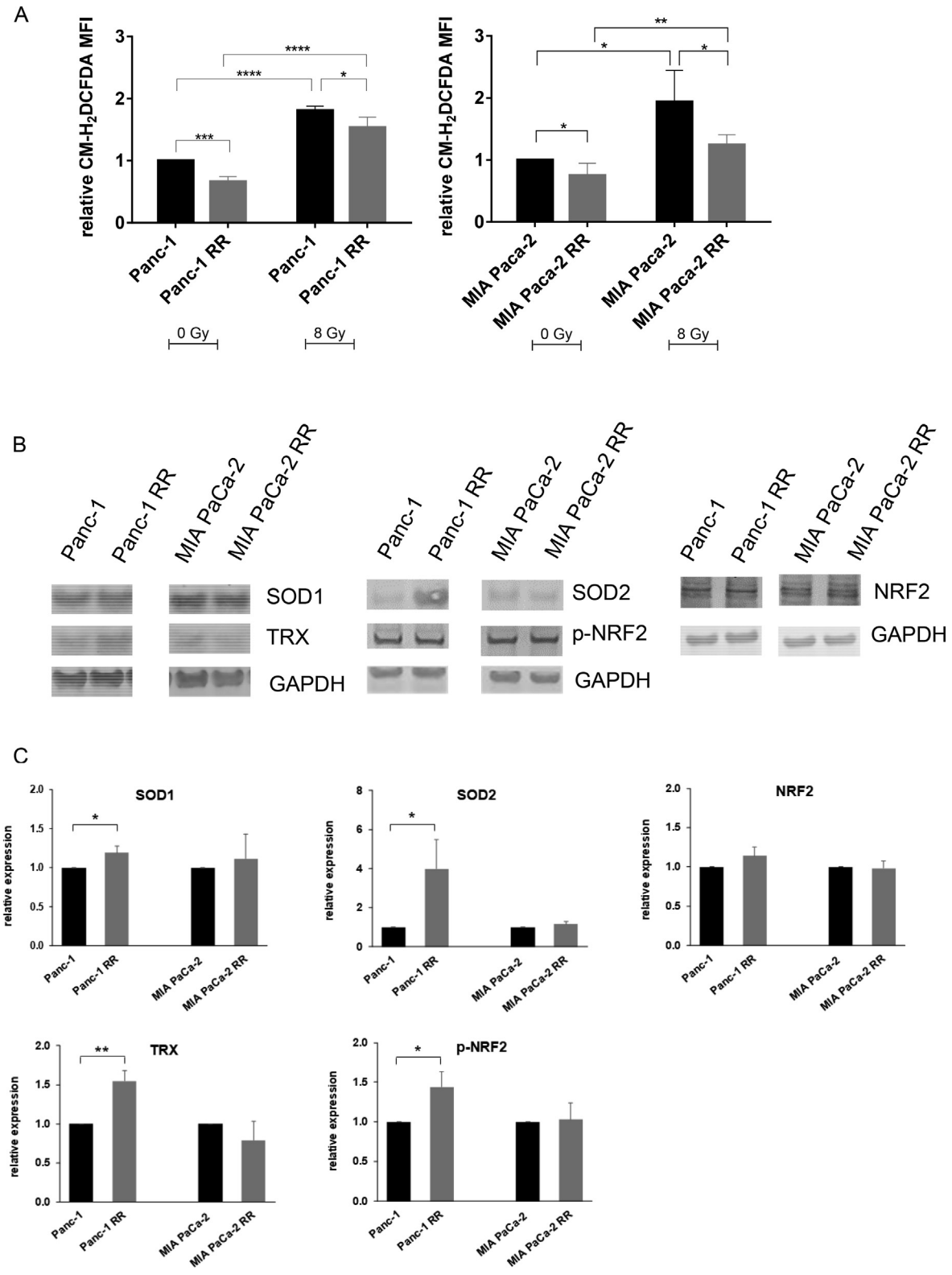

Fig. 5. X-Ray-induced oxidative stress is reduced in radioresistant (RR) cell lines. A. Intracellular reactive oxygen species were measured by CM–H_2DCFDA and flow cytometry immediately after irradiation with 8 Gy. Unirradiated cells (0 Gy) served as a control. MFI values for each cell line were normalized to the MFI obtained for the respective unirradiated parental cell lines. Data are expressed as mean ± SD of at least 3 independent experiments (Student's t-test; $^{*}p \leq 0.05$, $^{**}p \leq 0.01$, $^{***}p \leq 0.001$, $^{****}p \leq 0.0001$). **B.** Representative Western blot showing the expression of SOD1, TRX, SOD2, p-NRF2 and NRF2 in parental and RR Panc-1 and MIA PaCa-2 cells. **C.** Quantification of Western blot analysis. ImageJ was used to quantify the bands in relation to the loading control GAPDH. The graph represents the quantification of proteins relative to GAPDH and normalized to the respective parental cell line. Data are expressed as mean ± SD of 3 independent experiments (Student's t-test; $^{*}p \leq 0.05$, $^{**}p \leq 0.01$).

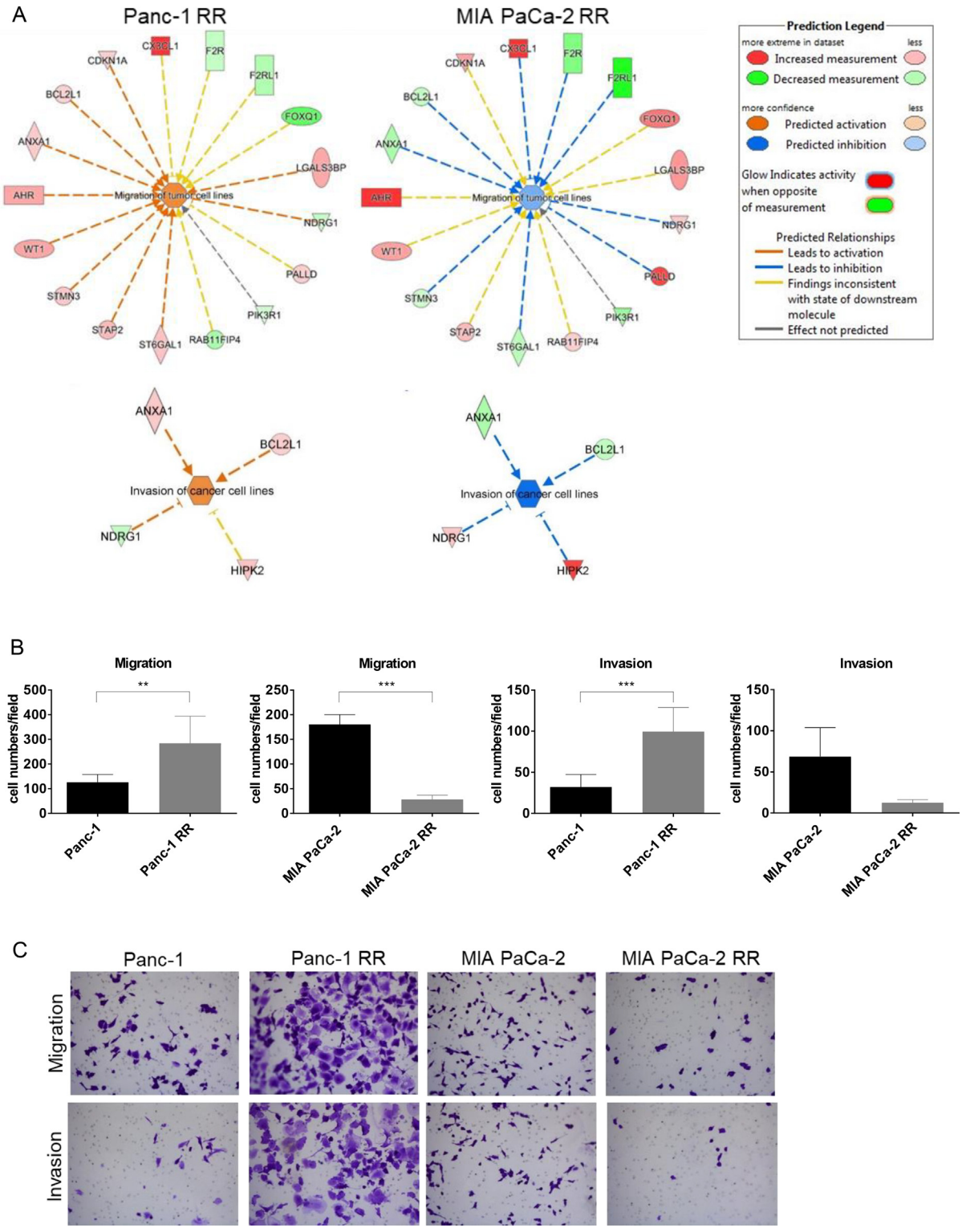

Fig. 6. RR cells show different migration and invasion capacities. A. IPA prediction of the activation of migration and invasion in Panc-1 RR cells and the inactivation in MIA PaCa-2 RR cells based on the shared deregulated genes from RNA sequencing between parental and RR cell lines. The upregulated genes are marked in red and the down-regulated genes in green. The orange color of the nodes indicates activation, whereas the blue color of the nodes indicates inactivation. The gene IDs and log2 fold change are available in Table S5. **B.** Migration and invasion capacity of parental and RR Panc–1 and MIA PaCa–2 cells were determined by transwell assay. Data are expressed as mean ± SD of at least 3 independent experiments (Student's t-test; $^{**}p \leq 0.01$, $^{***}p \leq 0.001$,). **C.** Representative images of transwell migration and invasion assays.

and the molecular mechanisms that lead to treatment failure are still unclear.

Therefore, in this study, isogenic radioresistant cell lines were created in order to investigate the mechanisms underlying radioresistance in pancreatic cancer. The selection of radioresistant subpopulations through repeated exposure to radiation has been previously reported in pancreatic cancer [26,39] and several other types of tumors including esophageal [40], prostate [41], and

breast [42]. It is important to mention that the RR cell lines in this study were not clonally derived; therefore, they represent a heterogeneous population, reflecting the heterogeneity seen in the clinic [43] and its implications for radioresistance [44].

In line with the acquired radioresistance *in vitro*, the RR cell line also maintained its radioresistant properties *in vivo*. After irradiation, tumors derived from RR cells showed a significantly shorter growth delay, i.e., an enhanced regrowth than parental tumors. Similar findings were previously reported in other mouse models of radioresistant cell lines [41].

In this study, mRNA sequencing and further analysis with the network-based analysis program, IPA, predicted enhanced cell viability in RR cell lines by the involvement of several deregulated genes which are known for their role in apoptosis, cell cycle distribution, DNA damage repair, and ROS generation [28–32].

In line with other reports, the induction of apoptosis after irradiation was analogous in both parental and radioresistant cells [40]. These findings indicate that other cell death mechanisms are more relevant in this model. In many tumors, apoptosis is not the major contributor to cell death [45]. Following DNA damage, cell death can occur in several ways, e.g., necrosis, mitotic catastrophe, and autophagy [45].

Cell cycle checkpoints are important determinants for the radio-responsiveness with the G2/M−phase being the most radiosensitive phase [46]. Surprisingly, the non-irradiated radioresistant cells revealed an accumulation in the G2/M phase. This unexpected finding was also reported by another group [40]. As our study showed comparable growth rates between parental and RR cell lines, a faster doubling time can be excluded as a reason. RNA sequencing and Western blot analysis revealed that the expression of p21 (CDKN1A) – a cyclin-dependent kinase inhibitor which has multiple functions in cell cycle regulation [47] – is increased in RR cell lines. p21 is a downstream target of p53 and its expression is induced by wild-type p53, but is not associated with mutant p53 [48]. As both parental cell lines, Panc-1 and MIA PaCa-2, harbor a p53 mutation [25], upregulation of p21 by p53 can be excluded. However, other mechanisms (e.g. epigenetic modifications, miRNAs, lncRNAs) leading to p21 upregulation in p53-mutated cancer cells have been described [47] and might contribute to increased p21 expression in the radioresistant cell lines. In line with our data, increased p21 expression protected lung cancer cells against the cytotoxic effect of radiation [49] and reduced p21 expression has been demonstrated to increase the radiosensitivity of gliomas, cervical cancer and colon cancer cells [50–53].

Besides p21, CDC2 (CDK1), Cyclin B1, CDC25C and WEE1 are important players controlling G2/M cell cycle checkpoint [54]. The transition from G2- to M-phase is mediated by activation of the CDC2-Cyclin B1 complex. While CDC25C activates CDC2, WEE1 and p21 inhibit CDC2 activity. We observed diminished expression of CDC25C, CDC2 and Cyclin B1 in radioresistant Panc-1 and MIA PaCa-2 cells which might explain the increased G2/M arrest in the radioresistant cell lines.

Irradiation induces a G2/M arrest during which DNA damage repair is promoted and thereby cells are protected from permanent genetic damage after ionizing radiation [19]. In our study, the radiation-induced G2/M arrest was attenuated in RR Panc-1 and MIA PaCa-2 cells compared to the parental cells. In line with our data, a reduced G2/M arrest after radiation has been observed in radioresistant nasopharyngeal cancer cells [55]. These findings indicate that the radioresistant cell lines have less radiation-induced DNA damage or a more efficient DNA repair capacity and therefore the radiation-induced G2/M arrest is less pronounced.

This was confirmed by our data showing that the radioresistant cell lines are less sensitive to initial DNA DSB induction after radiation and have an increased ability to repair DNA damage. Comparable results are well documented in other models of radioresistant cell lines, derived from repeated exposure to radiation [40,56]. Furthermore, RNA sequencing revealed upregulation of aryl hydrogen receptor (*AHR*) in the radioresistant cell lines. This is in line with the implication of AHR in the DNA DSB repair [32]. Thus, our data suggest that the acquired radioresistance might be due to the improved DNA damage response and repair.

Aside from the enhanced DNA repair capacity, the radioresistant Panc-1 and MIA PaCa-2 cell lines revealed lower basal and radiation-induced ROS levels. In line with our data, Cojoc et al. showed lower basal ROS levels in RR prostate cancer cells compared to the parental cells [41]. Furthermore, it was reported that a radioresistant non-small cell lung cancer cell line that also has been established by fractionated radiation showed decreased radiation-induced ROS levels compared to its parental cell line [57]. ROS are well known to play a role in the induction of genomic instability after radiation and are crucial mediators for DNA damage [58,59]. Therefore, reduced ROS levels indicate less oxidative stress and may explain the radioresistant phenotype of MIA PaCa-2 RR and Panc-1 RR cell lines. Furthermore, in Panc-1 RR cells upregulation of SOD1, SOD2, p-NRF2 and TRX was observed. In line with our data, SOD1 overexpression enhanced the radioresistance of glioma cells and suppressed the accumulation of radiation-induced ROS [60]. Another group observed an upregulation of SOD2 in a radioresistant nasopharyngeal carcinoma lineage and its association with radioresistance [61]. The cellular antioxidant response is primarily regulated by the transcription factor NRF2 [62]. When NRF2 is phosphorylated, p-NRF2 translocates to the nucleus and activates the expression of several other antioxidant genes, including SOD1 and SOD2 [63,64]. Therefore, increased levels of p-NRF2 may be the reason for the SOD1 and SOD2 upregulation in Panc-1 RR cells. Furthermore, the redox homeostasis is preserved by thioredoxin (TRX), a protein that reduces ROS by cysteine thiol-disulfide exchange. *In vitro* experiments in human breast and pancreatic cancer cell lines showed an enhanced response to irradiation by a combined inhibition of the TRX and glutathione metabolism [65]. This corresponds to our data demonstrating increased TRX expression in Panc-1 RR cells.

One feature of pancreatic cancer is its fast progression to metastatic disease and the associated poor prognosis; therefore, further understanding of the mechanisms leading to metastasis is of clinical importance. IPA analysis of our RNA sequencing data predicted differential invasion and migration capacity in Panc−1 RR and MIA PaCa−2 RR cells mainly due to the deregulation of *ANXA1, BCL2L1,* and *NDRG1*. These genes are well-known for their role in migration and invasion [66–68]. A high expression of annexin A1 (ANXA1) is associated with higher invasiveness and poorer survival in pancreatic cancer patients and ANXA1 knockdown has been shown to decrease migration and invasion [67,69–71]. Whereas overexpression of BCL2L1 enhanced migration and invasion in melanoma and glioblastoma cells [72], overexpression of NDRG1 in pancreatic cancer cell lines was associated with decreased invasion capacity [73]. In line with these studies, we showed increased migration and invasion ability in the Panc−1 RR cell line but decreased migration and invasion in the MIA PaCa−2 RR cell line. While the more aggressive phenotype seen in the Panc−1 RR cell line was also reported in other studies [41], this is to our knowledge the first report of a decreased migration and invasion ability in a radioresistant cell line. Further investigation of this different behavior in the two RR cell lines might warrant new insights into the progression of pancreatic cancer to metastatic disease.

In summary, our data suggest that reduced levels of ROS and improved DNA repair mechanisms might contribute to the acquired radioresistance in RR cells. However, migration and invasion capability were differently affected in the two RR cell lines. Whereas one RR cell line showed a decrease in migration and inva-

sion, the other RR cell line exhibited a more aggressive phenotype with enhanced migratory and invasive characteristics.

The results of the present work are a solid basis for further investigations potentially paving the road to a patient-specific biomarker discriminating radiosensitive from radioresistant tumors, which will potentially lead to a selective application of radiotherapy in pancreatic cancer patients. With this strategy, the real benefit of radiotherapy may be exploited effectively while preventing overtreatment in patients with radioresistant tumors.

Declaration of Competing Interest

Prof. Combs reports grants from Deutsche Forschungsgemeinschaft, non-financial support from Deutsches Konsortium für Translationale Krebsforschung, during the conduct of the study; personal fees and non-financial support from Roche, personal fees and non-financial support from AstraZeneca, personal fees and non-financial support from Medac, personal fees and nonfinancial support from Dr. Sennewald Medizintechnik, personal fees and non-financial support from Elekta, personal fees and non-financial support from Accuray, personal fees and nonfinancial support from BMS, personal fees and non-financial support from Brainlab, personal fees and non-financial support from Daiichi Sankyo, personal fees and non-financial support from Icotec, outside the submitted work.

Acknowledgements

The authors thank Marlon Stein for excellent technical assistance.

This work was funded by Deutsche Forschungsgemeinschaft (DFG, German Research Foundation) – Projektnummer 329628492 – SFB 1321 as well as the Deutsches Konsortium für Translationale Krebsforschung (DKTK), Partner Site Munich, and the School of Medicine, Technical University of Munich, within the KKF Grant Funding and the Hans and Klementia Langmatz Stiftung.

Appendix A. Supplementary data

Supplementary data to this article can be found online at https://doi.org/10.1016/j.radonc.2021.03.038.

References

[1] Carrato A, Falcone A, Ducreux M, Valle JW, Parnaby A, Djazouli K, et al. A systematic review of the burden of pancreatic cancer in Europe: Real-world impact on survival, quality of life and costs. J Gastrointest Cancer 2015;46 (3):201–11.
[2] Siegel RL, Miller KD, Jemal A. Cancer statistics, 2017. CA Cancer J Clin 2017;67 (1):7–30.
[3] Rahib L, Smith BD, Aizenberg R, Rosenzweig AB, Fleshman JM, Matrisian LM. Projecting cancer incidence and deaths to 2030: the unexpected burden of thyroid, liver, and pancreas cancers in the United States. Cancer Res 2014;74 (11):2913–21.
[4] Gillen S, Schuster T, Meyer Zum Buschenfelde C, Friess H, Kleeff J. Preoperative/neoadjuvant therapy in pancreatic cancer: a systematic review and meta-analysis of response and resection percentages. PLoS Med 2010;7: e1000267.
[5] Combs SE, Habermehl D, Werner J, Buchler MW, Debus J. Strategies for preoperative downsizing in patients with local nonresectable pancreatic cancer. Der Chirurg; Zeitschrift fur alle Gebiete der operativen Medizen 2011;82:981–8.
[6] Werner J, Combs SE, Springfeld C, Hartwig W, Hackert T, Büchler MW. Advanced-stage pancreatic cancer: therapy options. Nat Rev Clin Oncol 2013;10(6):323–33.
[7] Diener MK, Combs SE, Büchler MW. Chemoradiotherapy for locally advanced pancreatic cancer. Lancet Oncol 2013;14(4):269–70.
[8] Seshacharyulu P, Baine MJ, Souchek JJ, Menning M, Kaur S, Yan Y, et al. Biological determinants of radioresistance and their remediation in pancreatic cancer. Biochim Biophys Acta, Rev Cancer 2017;1868(1):69–92.
[9] Neoptolemos JP, Baker P, Beger H, Link K, Pederzoli P, Bassi C, et al. Progress report. A randomized multicenter European study comparing adjuvant radiotherapy, 6-mo chemotherapy, and combination therapy vs no-adjuvant treatment in resectable pancreatic cancer (ESPAC-1). Int J Pancreatol 1997;21:97–104.
[10] Murphy JE, Wo JY, Ryan DP, Jiang W, Yeap BY, Drapek LC, et al. Total neoadjuvant therapy With FOLFIRINOX followed by individualized chemoradiotherapy for borderline resectable pancreatic adenocarcinoma: A phase 2 clinical trial. JAMA Oncol 2018;4(7):963. https://doi.org/10.1001/jamaoncol.2018.0329.
[11] Cardenes HR, Moore AM, Johnson CS, Yu M, Helft P, Chiorean EG, et al. A phase II study of gemcitabine in combination with radiation therapy in patients with localized, unresectable, pancreatic cancer: a Hoosier Oncology Group study. Am J Clin Oncol 2011;34:460–5.
[12] McGinn CJ, Zalupski MM, Shureiqi I, Robertson JM, Eckhauser FE, Smith DC, et al. Phase I trial of radiation dose escalation with concurrent weekly full-dose gemcitabine in patients with advanced pancreatic cancer. J Clin Oncol 2001;19 (22):4202–8.
[13] Murphy JD, Adusumilli S, Griffith KA, Ray ME, Zalupski MM, Lawrence TS, et al. Full-dose gemcitabine and concurrent radiotherapy for unresectable pancreatic cancer. Int J Radiat Oncol Biol Phys 2007;68(3):801–8.
[14] Wolff RA, Evans DB, Gravel DM, Lenzi R, Pisters PW, Lee JE, et al. Phase I trial of gemcitabine combined with radiation for the treatment of locally advanced pancreatic adenocarcinoma. Clin Cancer Res 2001;7:2246–53.
[15] Combs SE. Individualized radiotherapy (iRT) concepts for locally advanced pancreatic cancer (LAPC): indications and prognostic factors. Langenbeck's Archiv Surg/Deutsche Gesellschaft fur Chirurgie 2015;400 (7):749–56.
[16] Dobiasch S, Goerig NL, Fietkau R, Combs SE. Essential role of radiation therapy for the treatment of pancreatic cancer : Novel study concepts and established treatment recommendations. Strahlentherapie und Onkologie : Organ der Deutschen Rontgengesellschaft [et al]. 2018;194:185-95.
[17] Barcellos-Hoff MH, Park C, Wright EG. Radiation and the microenvironment - tumorigenesis and therapy. Nat Rev Cancer 2005;5(11):867–75.
[18] Baskar R, Dai J, Wenlong N, Yeo R, Yeoh KW. Biological response of cancer cells to radiation treatment. Front Mol Biosci 2014;1:24.
[19] Kastan MB, Bartek J. Cell-cycle checkpoints and cancer. Nature 2004;432 (7015):316–23.
[20] Bauman JE, Chung CH. CHK it out! Blocking WEE kinase routs TP53 mutant cancer. Clin Cancer Res 2014;20(16):4173–5.
[21] Trachootham D, Alexandre J, Huang P. Targeting cancer cells by ROS-mediated mechanisms: a radical therapeutic approach?. Nat Rev Drug Discov 2009;8 (7):579–91.
[22] Giaccia AJ, Schwartz J, Shieh J, Brown JM. The use of asymmetric-field inversion gel electrophoresis to predict tumor cell radiosensitivity. Radiother Oncol 1992;24(4):231–8.
[23] Hosoya N, Miyagawa K. Targeting DNA damage response in cancer therapy. Cancer Sci 2014;105:370–88.
[24] Raza MH, Siraj S, Arshad A, Waheed U, Aldakheel F, Alduraywish S, et al. ROS-modulated therapeutic approaches in cancer treatment. J Cancer Res Clin Oncol 2017;143(9):1789–809.
[25] Moore PS, Sipos B, Orlandini S, Sorio C, Real FX, Lemoine NR, et al. Genetic profile of 22 pancreatic carcinoma cell lines. Analysis of K-ras, p53, p16 and DPC4/Smad4. Virchows Archiv 2001;439(6):798–802.
[26] Wang P, Zhang J, Zhang Li, Zhu Z, Fan J, Chen L, et al. MicroRNA 23b regulates autophagy associated with radioresistance of pancreatic cancer cells. Gastroenterology 2013;145(5):1133–1143.e12.
[27] Tanaka T, Halicka D, Traganos F, Darzynkiewicz Z. Cytometric analysis of DNA damage: phosphorylation of histone H2AX as a marker of DNA double-strand breaks (DSBs). Methods Mol Biol 2009;523:161–8.
[28] Yeo D, He H, Baldwin GS, Nikfarjam M. The role of p21-activated kinases in pancreatic cancer. Pancreas 2015;44:363–9.
[29] Feng Y, Zhou L, Sun X, Li Qi. Homeodomain-interacting protein kinase 2 (HIPK2): a promising target for anti-cancer therapies. Oncotarget 2017;8 (12):20452–61.
[30] Chen Y-J, Lin C-P, Hsu M-L, Shieh H-R, Chao NK, Chao KSC. Sonic hedgehog signaling protects human hepatocellular carcinoma cells against ionizing radiation in an autocrine manner. Int J Radiat Oncol Biol Phys 2011;80 (3):851–9.
[31] Yu Z, Zhang C, Wang H, Xing J, Gong H, Yu E, et al. Multidrug resistance-associated protein 3 confers resistance to chemoradiotherapy for rectal cancer by regulating reactive oxygen species and caspase-3-dependent apoptotic pathway. Cancer Lett 2014;353(2):182–93.
[32] Dittmann KH, Rothmund MC, Paasch A, Mayer C, Fehrenbacher B, Schaller M, et al. The nuclear aryl hydocarbon receptor is involved in regulation of DNA repair and cell survival following treatment with ionizing radiation. Toxicol Lett 2016;240(1):122–9.
[33] Abbas T, Dutta A. p21 in cancer: intricate networks and multiple activities. Nat Rev Cancer 2009;9(6):400–14.
[34] Habermehl D, Kessel K, Welzel T, Hof H, Abdollahi A, Bergmann F, et al. Neoadjuvant chemoradiation with Gemcitabine for locally advanced pancreatic cancer. Radiat Oncol 2012;7(1). https://doi.org/10.1186/1748-717X-7-28.
[35] Combs SE, Habermehl D, Kessel K, Bergmann F, Werner J, Brecht I, et al. Intensity modulated radiotherapy as neoadjuvant chemoradiation for the treatment of patients with locally advanced pancreatic cancer. Outcome analysis and comparison with a 3D-treated patient cohort. Strahlentherapie und Onkologie : Organ der Deutschen Rontgengesellschaft [et al]. 2013;189:738-44.
[36] Combs SE, Habermehl D, Kessel KA, Bergmann F, Werner J, Naumann P, et al. Prognostic impact of CA 19–9 on outcome after neoadjuvant chemoradiation

in patients with locally advanced pancreatic cancer. Ann Surg Oncol 2014;21 (8):2801–7.
[37] Hazard L, Tward JD, Szabo A, Shrieve DC. Radiation therapy is associated with improved survival in patients with pancreatic adenocarcinoma: results of a study from the Surveillance, Epidemiology, and End Results (SEER) registry data. Cancer 2007;110(10):2191–201.
[38] Campbell F, Smith RA, Whelan P, Sutton R, Raraty M, Neoptolemos JP, et al. Classification of R1 resections for pancreatic cancer: the prognostic relevance of tumour involvement within 1 mm of a resection margin. Histopathology 2009;55:277–83.
[39] Souchek JJ, Baine MJ, Lin C, Rachagani S, Gupta S, Kaur S, et al. Unbiased analysis of pancreatic cancer radiation resistance reveals cholesterol biosynthesis as a novel target for radiosensitisation. Br J Cancer 2014;111 (6):1139–49.
[40] Lynam-Lennon N, Reynolds JV, Pidgeon GP, Lysaght J, Marignol L, Maher SG. Alterations in DNA repair efficiency are involved in the radioresistance of esophageal adenocarcinoma. Radiat Res 2010;174(6a):703–11.
[41] Cojoc M, Peitzsch C, Kurth I, Trautmann F, Kunz-Schughart LA, Telegeev GD, et al. Aldehyde dehydrogenase is regulated by beta-catenin/TCF and promotes radioresistance in prostate cancer progenitor cells. Cancer Res 2015;75:1482–94.
[42] Wang T, Tamae D, LeBon T, Shively JE, Yen Y, Li JJ. The role of peroxiredoxin II in radiation-resistant MCF-7 breast cancer cells. Cancer Res 2005;65 (22):10338–46.
[43] Cros J, Raffenne J, Couvelard A, Poté N. Tumor heterogeneity in pancreatic adenocarcinoma. Pathobiology 2018;85(1-2):64–71.
[44] Weichselbaum RR, Beckett MA, Dahlberg W, Dritschilo A. Heterogeneity of radiation response of a parent human epidermoid carcinoma cell line and four clones. Int J Radiat Oncol Biol Phys 1988;14(5):907–12.
[45] Brown JM, Attardi LD. The role of apoptosis in cancer development and treatment response. Nat Rev Cancer 2005;5(3):231–7.
[46] Pawlik TM, Keyomarsi K. Role of cell cycle in mediating sensitivity to radiotherapy. Int J Radiat Oncol Biol Phys 2004;59(4):928–42.
[47] Ocker M, Bitar SA, Monteiro AC, Gali-Muhtasib H, Schneider-Stock R. Epigenetic regulation of p21(cip1/waf1) in human cancer. Cancers 2019;11 (9):1343. https://doi.org/10.3390/cancers11091343.
[48] Xiao B-D, Zhao Y-J, Jia X-Y, Wu J, Wang Y-G, Huang F. Multifaceted p21 in carcinogenesis, stemness of tumor and tumor therapy. World J Stem Cells 2020;12(6):481–7.
[49] Wang Y, Blandino G, Givol D. Induced p21waf expression in H1299 cell line promotes cell senescence and protects against cytotoxic effect of radiation and doxorubicin. Oncogene 1999;18(16):2643–9.
[50] Kokunai T, Urui S, Tomita H, Tamaki N. Overcoming of radioresistance in human gliomas by p21WAF1/CIP1 antisense oligonucleotide. J Neurooncol 2001;51:111–9.
[51] Pedroza Torres A, Campos Parra A, Millan Catalan O, Loissell Baltazar Y, Zamudio Meza H, Cantu de Leon D, et al. MicroRNA-125 modulates radioresistance through targeting p21 in cervical cancer. Oncol Rep 2018. https://doi.org/10.3892/or10.3892/or.2018.6219.
[52] Tian H, Wittmack EK, Jorgensen TJ. p21WAF1/CIP1 antisense therapy radiosensitizes human colon cancer by converting growth arrest to apoptosis. Cancer Res 2000;60:679–84.
[53] Wouters BG, Giaccia AJ, Denko NC, Brown JM. Loss of p21Waf1/Cip1 sensitizes tumors to radiation by an apoptosis-independent mechanism. Cancer Res 1997;57:4703–6.
[54] Castedo M, Perfettini J-L, Roumier T, Kroemer G. Cyclin-dependent kinase-1: linking apoptosis to cell cycle and mitotic catastrophe. Cell Death Differ 2002;9(12):1287–93.
[55] Peng Y, Fu S, Hu W, Qiu Y, Zhang Lu, Tan R, et al. Glutamine synthetase facilitates cancer cells to recover from irradiation-induced G2/M arrest. Cancer Biol Ther 2020;21(1):43–51.
[56] McDermott N, Meunier A, Mooney B, Nortey G, Hernandez C, Hurley S, et al. Fractionated radiation exposure amplifies the radioresistant nature of prostate cancer cells. Sci Rep 2016;6(1). https://doi.org/10.1038/srep34796.
[57] Lee YS, Oh J-H, Yoon S, Kwon M-S, Song C-W, Kim K-H, et al. Differential gene expression profiles of radioresistant non-small-cell lung cancer cell lines established by fractionated irradiation: tumor protein p53-inducible protein 3 confers sensitivity to ionizing radiation. Int J Radiat Oncol Biol Phys 2010;77 (3):858–66.
[58] Sasano N, Enomoto A, Hosoi Y, Katsumura Y, Matsumoto Y, Shiraishi K, et al. Free radical scavenger edaravone suppresses x-ray-induced apoptosis through p53 inhibition in MOLT-4 cells. J Radiat Res 2007;48(6):495–503.
[59] Wang H, Bouzakoura S, de Mey S, Jiang H, Law K, Dufait I, et al. Auranofin radiosensitizes tumor cells through targeting thioredoxin reductase and resulting overproduction of reactive oxygen species. Oncotarget 2017;8 (22):35728–42.
[60] Gao Z, Sarsour EH, Kalen AL, Li L, Kumar MG, Goswami PC. Late ROS accumulation and radiosensitivity in SOD1-overexpressing human glioma cells. Free Radical Biol Med 2008;45(11):1501–9.
[61] Feng X-P, Yi H, Li M-Y, Li X-H, Yi B, Zhang P-F, et al. Identification of biomarkers for predicting nasopharyngeal carcinoma response to radiotherapy by proteomics. Cancer Res 2010;70(9):3450–62.
[62] Rojo de la Vega M, Chapman E, Zhang DD. NRF2 and the hallmarks of cancer. Cancer Cell 2018;34(1):21–43.
[63] Basak P, Sadhukhan P, Sarkar P, Sil PC. Perspectives of the Nrf-2 signaling pathway in cancer progression and therapy. Toxicol Rep 2017;4:306–18.
[64] He F, Ru X, Wen T. NRF2, a transcription factor for stress response and beyond. Int J Mol Sci 2020;21(13):4777. https://doi.org/10.3390/ijms21134777.
[65] Rodman SN, Spence JM, Ronnfeldt TJ, Zhu Y, Solst SR, O'Neill RA, et al. Enhancement of radiation response in breast cancer stem cells by inhibition of thioredoxin- and glutathione-dependent metabolism. Radiat Res 2016;186 (4):385. https://doi.org/10.1667/RR14463.110.1667/RR14463.1.s1.
[66] Um H-D. Bcl-2 family proteins as regulators of cancer cell invasion and metastasis: a review focusing on mitochondrial respiration and reactive oxygen species. Oncotarget 2016;7(5):5193–203.
[67] Belvedere R, Bizzarro V, Forte G, Dal Piaz F, Parente L, Petrella A. Annexin A1 contributes to pancreatic cancer cell phenotype, behaviour and metastatic potential independently of Formyl Peptide Receptor pathway. Sci Rep 2016;6:29660.
[68] Maruyama Y, Ono M, Kawahara A, Yokoyama T, Basaki Y, Kage M, et al. Tumor growth suppression in pancreatic cancer by a putative metastasis suppressor gene Cap43/NDRG1/Drg-1 through modulation of angiogenesis. Cancer Res 2006;66(12):6233–42.
[69] Chen C-Y, Shen J-Q, Wang F, Wan R, Wang X-P. Prognostic significance of annexin A1 expression in pancreatic ductal adenocarcinoma. Asian Pacific J Cancer Prevent APJCP 2012;13(9):4707–12.
[70] Bai XF, Ni XG, Zhao P, Liu SM, Wang HX, Guo B, et al. Overexpression of annexin 1 in pancreatic cancer and its clinical significance. World J Gastroenterol 2004;10:1466–70.
[71] Belvedere R, Bizzarro V, Popolo A, Dal Piaz F, Vasaturo M, Picardi P, et al. Role of intracellular and extracellular annexin A1 in migration and invasion of human pancreatic carcinoma cells. BMC Cancer 2014;14(1). https://doi.org/10.1186/1471-2407-14-961.
[72] Trisciuoglio D, Tupone MG, Desideri M, Di Martile M, Gabellini C, Buglioni S, et al. BCL-XL overexpression promotes tumor progression-associated properties. Cell Death Dis 2017;8(12). https://doi.org/10.1038/s41419-017-0055-y.
[73] Cen G, Zhang K, Cao J, Qiu Z. Downregulation of the N-myc downstream regulated gene 1 is related to enhanced proliferation, invasion and migration of pancreatic cancer. Oncol Rep 2017;37:1189–95.